Acta Biochim Biophys Sin (2008): 565-576 | © 2008 Institute of Biochemistry and Cell Biology, SIBS, CAS | All Rights Reserved 1672-9145
http://www.abbs.info; www.blackwellpublishing.com/abbs | DOI: 10.1111/j.1745-7270.2008.00437.x

Review

Applications of isothermal titration calorimetry in protein science

Yi Liang*

State Key Laboratory of Virology, College of Life Sciences, Wuhan University, Wuhan 430072, China

During the past decade, isothermal titration calorimetry (ITC) has developed from a specialist method for understanding molecular interactions and other biological processes within cells to a more robust, widely used method. Nowadays, ITC is used to investigate all types of protein interactions, including protein-protein interactions, protein-DNA/RNA interactions, protein-small molecule interactions and enzyme kinetics; it provides a direct route to the complete thermodynamic characterization of protein interactions. This review concentrates on the new applications of ITC in protein folding and misfolding, its traditional application in protein interactions, and an overview of what can be achieved in the field of protein science using this method and what developments are likely to occur in the near future. Also, this review discusses some new developments of ITC method in protein science, such as the reverse titration of ITC and the displacement method of ITC.

Keywords isothermal titration calorimetry; protein folding; protein misfolding; protein interaction; thermodynamics

Isothermal titration calorimetry (ITC), which provides a direct route to the complete thermodynamic characterization of protein interactions, has been one of the fastest developing techniques in protein science research in the past decade [1–4]. A syringe of ITC containing a ligand is titrated into a cell containing a protein solution. As the two elements interact, heat is released or absorbed in direct proportion to the amount of binding that occurs. When the protein in the cell becomes saturated with the added ligand, the heat signal diminishes until only the background heat of dilution is observed. Measurement of this heat allows for the accurate determination of binding constants (K_b), reaction stoichiometry (n), and a thermodynamic profile of the protein interaction that includes the observed molar calorimetric enthalpy (ΔH_{obs}), entropy (ΔS_{obs}), heat capacity ($\Delta C_{p,obs}$) of binding and change in free energy (ΔG). Unlike other methods, ITC does not require immobilization and/or modification of proteins since the absorption or production of heat is an intrinsic property of virtually all biochemical reactions [1–4].

There are at least four reasons for the increasing popularity of ITC in the field of protein science: (1) the technique is relatively easy to perform, resulting in the generation of a large amount of thermodynamic data with only a small amount of protein; (2) in some instances, the K_b values of a series of protein interactions are similar or indistinguishable [5], however, the determination of the ΔH and ΔS terms allows a further level of discrimination; (3) although it is not possible to provide a full thermodynamic-structure correlation of proteins from an ITC experiment, it is possible to reach sensible conclusions from the data by comparing subtle conformational changes of proteins; (4) the correlation of the ΔC_p term with the change in surface area buried on forming a protein interface has proven to be a useful tool in understanding protein interactions with respect to both structure and thermodynamics [6,7]. ITC experiments performed at different temperatures provide an accurate, direct determination of the ΔC_p term. Thanks to the recent development of commercially available high-sensitivity instruments, for example the VP-ITC and iTC-200 titration calorimeters from MicroCal, there has been a revival of ITC in the field of protein science, which will help to provide a better understanding of the mechanisms for protein interactions in signal transduction [1–4].

Nowadays, ITC is used to investigate all types of protein interactions, including protein-protein interactions, protein-DNA/RNA interactions, protein-small molecule interactions

Received: May 3, 2008 Accepted: May 26, 2008
This work was supported by grants from the National Key Basic Research Foundation of China (No. 2006CB910301), the National Natural Science Foundation of China (No. 30770421) and the Program for New Century Excellent Talents in University (No. NCET-04-0670)
*Corresponding author: Tel/Fax, 86-27-68754902; E-mail, liangyi@whu.edu.cn

and enzyme kinetics, and it provides a direct route to the complete thermodynamic characterization of protein interactions. The following reviews the new applications for ITC in protein folding and misfolding, as well as its traditional application in protein interactions. Additionally, this review provides an overview of what can be achieved in the field of protein science using this method and what developments are likely to occur in the near future. Some new ITC developments in protein science, such as the reverse titration of ITC and the displacement method of ITC, are also discussed.

ITC Applications in Protein Folding and Misfolding

Although the principles that govern the folding of protein chains have been widely discussed since the pioneering studies of Anfinsen [8], knowledge about the thermodynamics of protein folding and misfolding from ITC is relatively limited. By virtue of its general applicability and high precision, ITC is a powerful tool for studying both the thermodynamic and kinetic properties of protein folding. This method combined with other biophysical methods has yielded some useful thermodynamic data on protein folding, assembly and misfolding [9–19]. Currently, ITC is being used to solve problems related to the important factors and the mechanisms involved in the formation and stability of amyloid fibrils in medical research. It is also being used to directly describe the thermodynamic properties of the folded form and the amyloid form of proteins [2,9,14].

In a previous study, my laboratory used ITC to examine the unfolding of rabbit muscle creatine kinase (MM-CK) induced by acid [9]. The results indicated that the unfolding of MM-CK under such conditions is driven by a favorable enthalpy change but with an unfavorable entropy decrease at lower temperatures (15 ºC) and becoming entropy-driven at higher temperatures (25 ºC, 30 ºC, and 37 ºC). The increase in $\Delta_{conf}H_m$, with increasing temperatures at pH 3.5 or 4.0, indicates that thermal unfolding occurs. The changes in enthalpy and entropy for the unfolding strongly depend on the temperature, whereas the Gibbs free energy change happens almost independent of temperature. The enthalpy change for the unfolding is almost compensated for by a corresponding change in entropy that results in a smaller net Gibbs free energy increase. That is, remarkable enthalpy-entropy compensation occurs in the acid-induced unfolding of the protein, suggesting that water reorganization is involved in the unfolding reaction. The value of $\Delta_U G_m^0$ for the unfolding of MM-CK induced by guanidine hydrochloride (6.24 kcal·mol^{-1}) is 2-fold of that induced by acid (3.37 kcal·mol^{-1}) [9,10], indicating that the protein is unfolded to a greater extent when induced by guanidine hydrochloride than when induced by acid [9]. Combining the results from ITC and other biophysical methods, we concluded that the acid-induced unfolding of MM-CK follows a three-state model and that the intermediate state of the protein is a partially folded monomer [9].

Isothermal acid-titration calorimetry (IATC) is a new method for evaluating the pH dependence of protein enthalpy. In a recent publication by Nakamura and Kidokoro [11], the enthalpy change accompanying the reversible acid-induced transition from the native to the molten-globule state of bovine cytochrome *c* was directly evaluated by this method. The results of the global analysis of the temperature dependence of the excess enthalpy from 20 ºC to 35 ºC have demonstrated that the native to molten-globule transition is a two-state transition with a small heat capacity change. Since protons naturally ligate to protein molecules [9], this new method is expected to be applicable to the thermodynamic evaluation of the stability of many kinds of proteins, without requiring temperature increases and without buffering reagent or denaturant [11].

The co-chaperonin protein 10 (cpn10) is a ring-shaped heptameric protein that exists in all organisms and whose function *in vivo* is to assist cpn60 in the folding of some non-native proteins. Luke and Wittung-Stafshede studied the assembly and disassembly of the *Escherichia coli* cpn10 (GroES) and *Aquifex aeolicus* cpn10 in the folded state using ITC and other biophysical methods [12]. Thermodynamic analysis revealed that *A. aeolicus* cpn10's stability profile is shifted upwards, broadened and moved horizontally to higher temperatures, as compared to that of GroES, and that cpn10's higher stability originates almost exclusively from increased monomer stability. Their study showed that protein biophysics can vary significantly among proteins with structural homology, and at the same time, it demonstrated that protein thermostability can be acquired without major changes in molecular properties [12].

Protein misfolding is of intense medical interest because it is associated with serious diseases, such as Alzheimer's disease, Parkinson's disease, transmissible spongiform encephalopathy and Huntington's disease [13]. Kardos *et al* have reported for the first time a direct thermodynamic study of amyloid formation using ITC [14]. In the study, β_2-microglobulin, a protein responsible for dialysis-related amyloidosis, was used for extending amyloid fibrils in a seed-controlled reaction in the cell of the calorimeter. The enthalpy and heat capacity changes of the reaction, where

the monomeric, acid-denatured molecules adopt an ordered, cross-β-sheet structure in the rigid amyloid fibrils, were investigated. Despite the dramatic difference in morphology, β_2-microglobulin has exhibited a similar heat capacity change upon amyloid formation as that of the folding on the native globular state, whereas the enthalpy change on the reaction has proved to be markedly lower. In comparison with the native state, the results outline the important structural features of the amyloid fibrils: a similar extent of surface burial even with the supramolecular architecture of amyloid fibrils, a lower level of internal packing, and the possible presence of unfavorable side chain contributions [14]. More importantly, in the absence of structural information on amyloid fibrils, the strategy used by Kardos *et al* in studying the thermodynamic formation of amyloid fibrils of β_2-microglobulin may become widely used in examining other protein systems in the formation of amyloids [14].

We studied the oxidative refolding of reduced, denatured hen egg-white lysozyme (HEL) in the presence of a mixed macromolecular crowding agent containing both bovine serum albumin (BSA) and polysaccharide from a physiological point of view [15]. Both the refolding yield and the rate of the oxidative refolding of lysozyme in these mixed crowded solutions with suitable weight ratios were higher than those in single crowded solutions, indicating that mixed macromolecular crowding agents are more favorable to lysozyme folding and can be used to reflect the physiological environment more accurately than single crowding agents [15,16]. We further investigated the effects of two single macromolecular crowding agents, Ficoll 70 and BSA, and one mixed macromolecular crowding agent containing both BSA and Ficoll 70 on amyloid formation of HEL as a function of crowder concentration and composition [17]. Both the mixed crowding agent and the protein crowding agent BSA (100 g/L) almost completely inhibited amyloid formation of lysozyme and stabilized lysozyme activity on the investigated time scale. However, 100 g/L Ficoll 70 neither effectively impeded amyloid formation of lysozyme nor stabilized lysozyme activity. By using ITC, we observed a weak, non-specific interaction between BSA and nonnative lysozyme at pH 2.0. The ITC results are shown in **Fig. 1(A,B)**. The best fit for the integrated heat data was obtained using a three sequential-binding sites model, yielding the thermodynamic parameters for the interaction between BSA and nonnative lysozyme: $K_{b,1}=(1.03\pm0.04)\times10^5$ M^{-1}, $\Delta_b H^0_{m,1}=-46.6\pm0.7$ kcal·mol^{-1}, $\Delta_b G^0_{m,1}=-7.12\pm0.10$ kcal·mol^{-1}, $\Delta_b S^0_{m,1}=-127\pm2$ cal·mol^{-1}·K^{-1}, $K_{b,2}=(1.01\pm0.04)\times10^5$ M^{-1}, $\Delta_b H^0_{m,2}=-6.1\pm1.5$ kcal·mol^{-1}·K^{-1}, $\Delta_b G^0_{m,2}=-7.11\pm0.11$ kcal·mol^{-1}, $\Delta_b S^0_{m,2}=3.2\pm4.6$ cal·mol^{-1}·K^{-1}, $K_{b,3}=(1.02\pm0.07)\times10^5$ M^{-1}, $\Delta_b H^0_{m,3}=-73.0\pm2.2$ kcal·mol^{-1}, $\Delta_b G^0_{m,3}=-7.11\pm0.12$ kcal·mol^{-1}, and $\Delta_b S^0_{m,3}=-213\pm7$ cal·mol^{-1}·K^{-1}. These results show that the binding of BSA to nonnative lysozyme is driven entirely by large favorable enthalpy decreases but with unfavorable entropy decreases for the first and the third sequential binding sites of nonnative lysozyme. This implies that BSA may bind to lysozyme oligomers to prevent the formation of prefibrillar lysozyme and bind with the protofibrils to retard fibril elongation of lysozyme. Furthermore, we performed ITC experiments on the binding of Ficoll 70 to nonnative lysozyme at pH 2.0 and found the calorimetric data too small to fit any binding model [**Fig. 1(C,D)**]. No optimal fit was found for Ficoll 70, indicating that it has no specific binding affinity for nonnative lysozyme under such experimental conditions. Our ITC analyses indicate that a mixture of 5 g/L BSA and 95 g/L Ficoll 70 inhibits amyloid formation of lysozyme and maintains both lysozyme activity via mixed macromolecular crowding and weak, nonspecific interactions between BSA and nonnative lysozyme [17]. Our data demonstrated that BSA and Ficoll 70 cooperatively contribute to both the inhibitory effect and the stabilization effect of the mixed crowding agent, suggesting that mixed macromolecular crowding inside the cell may play a role in posttranslational quality control mechanism [17].

α-synuclein is the vital protein involved in neurodegenerative diseases, such as Parkinson's disease. Amyloid formation of recombinant human α-synuclein *in vitro* can be accelerated by sodium dodecylsulfate (SDS). Ahmad *et al* employed ITC and other biophysical methods to characterize the protein-detergent interactions as a function of the concentration of SDS [18]. Their study showed two types of ensembles of α-synuclein and SDS: the fibrillogenic ensembles formed with optimal concentration of SDS around 0.5–0.75 mM, are characterized by enhanced accessible hydrophobic surfaces and extended to partially helical conformation, while the less or non-fibrillogenic ensembles formed above 2 mM SDS, are characterized by less accessible hydrophobic surfaces and maximal helical content [18]. Their study with the membrane-mimicking agent SDS should prove useful in understanding the role of amphiphilic molecules in the fibrillogenicity of α-synuclein.

Amyloid fibrils share various common structural features, and their presence can be detected by thioflavin T (ThT). Despite widespread use of ThT for identifying amyloid fibrils, the mode for binding ThT to amyloid fibrils is largely unknown. A detailed knowledge of the binding mode of ThT to amyloid fibrils is essential for

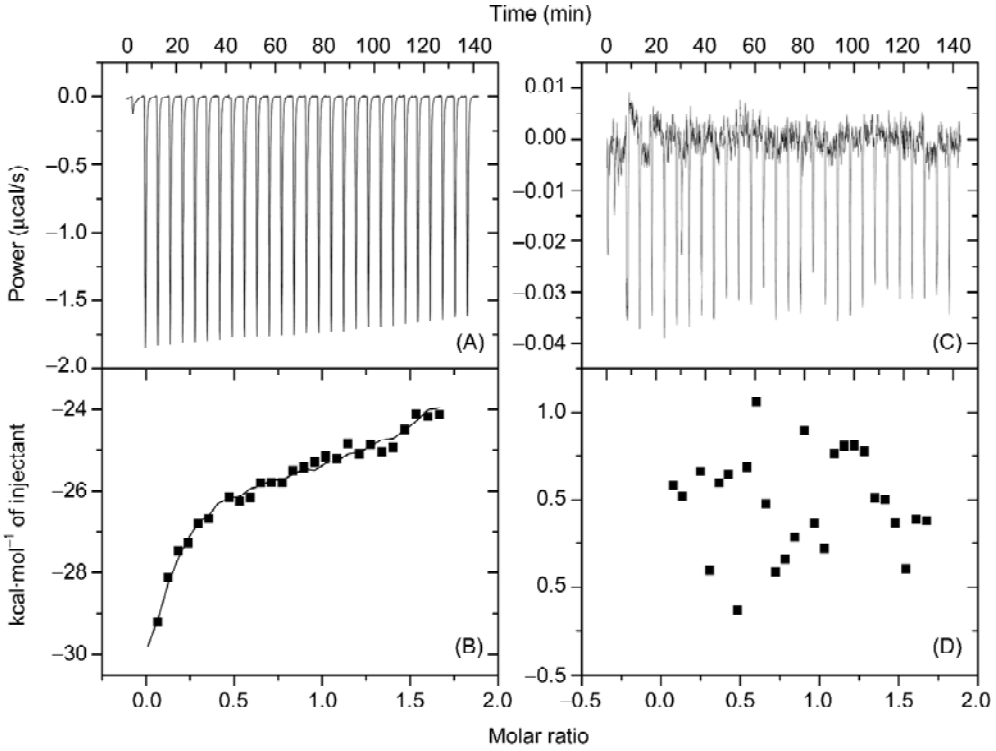

Fig. 1 Isothermal titration calorimetry profiles for the binding of bovine serum albumin (BSA) or Ficoll 70 to lysozyme samples at pH 2.0 after incubation for 10 d in the absence of crowding agents at 37 ºC (A) The raw data for sequential 10-μl injections of 139 μM BSA into17.4 μM lysozyme solution incubated for 10 d. The first injection was of 4 μl BSA. (B) The plot of the heat evolved (kcal) per mole of BSA added, corrected for the heat of BSA dilution, against the molar ratio of BSA to lysozyme incubated for 10 d. The data (filled squares) were fitted to a three sequential-binding sites model, and the solid lines represent the best fit. (C) The raw data for sequential 10-μl injections of 139 μM Ficoll 70 into 17.4 μM lysozyme solution incubated for 10 d. The first injection was of 4 μl Ficoll 70. (D) The plot of the heat evolved (kcal) per mole of Ficoll 70 added, corrected for the heat of Ficoll 70 dilution, against the molar ratio of Ficoll 70 to lysozyme incubated for 10 d. The data (filled square) were too small to fit, indicating that no binding was observed in the conditions used.

understanding the mechanism for protein misfolding. Groenning *et al* examined the binding mode of ThT to insulin amyloid fibrils using ITC and Scatchard analysis [19], and confirmed at least two binding site populations. The binding site population with the strongest binding is responsible for the characteristic ThT fluorescence. This binding has a capacity of about 0.1 moles of ThT bound per mole of insulin in fibril form. The binding capacity is unaffected by pH, but the affinity is lowest at low pH. Notably, the presence of a third binding process prior to the other processes is suggested by ITC [19].

ITC Applications in Protein-protein Interactions

Protein-protein interactions (PPI) play key roles in many essential biological processes, such as the regulation of enzymatic activities, the assembly of cellular components, and signal transduction [20]. ITC is the most quantitative means available for measuring the thermodynamic properties of PPI and is becoming a necessary tool for PPI complex structural studies [1–4,21–28].

Xanthine oxidase (XO) and copper, zinc superoxide dismutase (Cu,Zn-SOD) are function-related proteins *in vivo*. We studied thermodynamics of the interaction of bovine milk XO with bovine erythrocyte Cu,Zn-SOD using ITC [21]. The binding of XO to Cu,Zn-SOD was driven by a large favorable enthalpy decrease with a large unfavorable entropy reduction, and showed strong entropy-enthalpy compensation and weak temperature-dependence of Gibbs free energy change. An unexpected, large positive molar heat capacity change of the binding, 3.02 $kJ \cdot mol^{-1} \cdot K^{-1}$, at all temperatures examined suggests that either hydrogen bond or long-range electrostatic interaction is a major force for the binding. The large unfavorable change in entropy suggests that long-range electrostatic

forces do not play an important role in the binding. These results indicate that XO binds to Cu,Zn-SOD with high affinity and that hydrogen bond is a major force for the binding [21].

Botulinum neurotoxins are produced by *Clostridium botulinum* and cause the neuroparalytic syndrome of botulism. Jin *et al* reported the structure of receptor-binding domain of botulinum neurotoxin serotype B and the luminal domain of synaptotagmin II, which is the receptor of the neurotoxin [22]. Their ITC data show that the carboxy-terminal domain of the heavy chain of the neurotoxin binds tightly to the luminal domain of synaptotagmin II with stoichiometry 1:1 and is endothermic and entropy driven. The heat capacity for the interaction is approximately -326 cal·mol^{-1}·K^{-1}, which is consistent with a protein-protein interaction driven by the hydrophobic effect. ITC titration at pH 5.7, mimicking the acidic endosomal environment, produced no change on assembly thermodynamics, indicating that the pH change associated with toxin internalization unlikely affects the binding of the neurotoxin to its protein receptor [22].

The small ubiquitin-related modifier (SUMO) regulates a wide range of cellular processes by post-translational modification with one or a chain of SUMO molecules. Sumoylation is achieved by the sequential action of several enzymes in which the E2, Ubc9, transfers SUMO from the E1 to the target mostly with the help of an E3 enzyme. In this process, Ubc9 not only forms a thioester bond with SUMO, but it also interacts with SUMO non-covalently [23]. Knipscheer *et al* showed that this non-covalent interaction promotes the formation of short SUMO chains on targets, such as Sp100 and HDAC4 [23]. ITC was used to determine the affinity of the interaction between Ubc9 and SUMO1. For the interaction between Ubc9 and SUMO1, a K_d of 82±23 nM was determined. However, the heat exchange of the reaction for SUMO2 binding was too small to be measured by ITC. Thus, in the two systems, the balance of affinities is maintained in different ways, emphasizing that ubiquitin and SUMO are analogous, but not identical. Nevertheless, the actual mechanism for chain formation seems once again surprisingly similar between the ubiquitin and SUMO pathways [23].

Protein phosphatase 2A (PP2A) is a major protein serine/threonine phosphatase and is involved in many essential aspects of cellular physiology [24]. The small T antigen (ST) of DNA tumor virus SV40 facilitates cellular transformation by disrupting the functions of PP2A through a poorly defined mechanism. Chen *et al* depicted the mechanism of ST regulation of PP2A and quantitatively measured the binding affinities between ST and PP2A using ITC [24]. They constructed a model that combined the affinity data and structure features, and showed how ST may interfere with the normal functions of PP2A. ST has a lower binding affinity than B56 for the PP2A core enzyme. Consequently, ST does not efficiently displace B56 from PP2A holoenzymes *in vitro*. Notably, ST inhibits PP2A phosphatase activity through its N-terminal J domain. These findings suggest that ST may function mainly by inhibiting the phosphatase activity of the PP2A core enzyme and, to a lesser extent, by modulating assembly of the PP2A holoenzymes [24].

The recent finding of an interaction between calmodulin and the tobacco mitogen-activated protein kinase (MAPK) phosphatase-1 has established an important connection between Ca^{2+} signaling and the MAPK cascade, two of the most important signaling pathways in plant cells. Rainaldi *et al* characterized the binding of soybean calmodulin isoforms to synthetic peptides derived from the calmodulin binding domain of the tobacco MAPK phosphatase-1 [25]. Using ITC, they found that in the presence of Ca^{2+}, the peptides bind first to the C-terminal lobe of calmodulin with a nanomolar affinity, and at higher peptide concentrations, a second peptide binds to the N-terminal domain with lower affinity. Thermodynamic analyses also demonstrate that the formation of the peptide-bound complex with the Ca^{2+}-loaded calmodulin is driven by favorable binding enthalpy due to a combination of hydrophobic and electrostatic interactions [25].

Association of two proteins can be described as a two-step process, with the formation of an encounter complex followed by desolvation and the establishment of a tight complex. Kiel *et al* designed a set of mutants of the Ras effector protein Ral guanine nucleotide dissociation stimulator (RalGDS) with optimized electrostatic steering [26]. The results from ITC and other biophysical methods showed that the fastest binding RalGDS mutant, M26K, D47K,E54K, binds Ras 14-fold faster and 25-fold tighter than the wild type. Upon further formation of the final complex, the increased Coulombic interactions are probably counterbalanced by the cost of desolvation of charges, keeping the dissociation rate constant almost unchanged. This mechanism is also reflected by the mutual compensation of enthalpy and entropy changes quantified by ITC. The binding constants of the faster binding RalGDS mutants toward Ras are similar to those of Raf, the most prominent Ras effector, suggesting that the design methodology may be used to switch between signal transduction pathways [26].

ATP hydrolysis by the Hsp90 molecular chaperone requires a connected set of conformational switches

triggered by ATP binding to the N-terminal domain in the Hsp90 dimer. Hsp90 mutants that influence these conformational switches have strong effects on ATPase activity. ATPase activity is specifically regulated by Hsp90 co-chaperones, which directly influence the conformational switches. Using ITC and other biophysical methods, Siligardi *et al* analyzed the effect of Hsp90 mutations on the binding and ATPase regulation by the co-chaperones Aha1, Sti1, and Sba1 [27]. The ability of Sti1 to bind Hsp90 and arrest its ATPase activity was not affected by any of the mutants screened. Sba1 bound in the presence of AMP-PNP to wild type and ATPase hyperactive mutants with similar affinity, but it bound very weakly to hypoactive mutants despite their wild-type ATP affinity. Unexpectedly, in all cases, Sba1 bound to Hsp90 with a 1:2 molar stoichiometry. Analyses of complex formation with co-chaperone mixtures have shown that Aha1 and $p50^{cdc37}$ are able to bind Hsp90 simultaneously but without direct interaction. Sba1 and $p50^{cdc37}$ bind independently to Hsp90-AMP-PNP but not together. These data have indicated that Sba1 and Aha1 regulate Hsp90 by influencing the conformational state of the "ATP lid" and consequent N-terminal dimerization, whereas Sti1 does not [27].

Elucidation of the roles of the hydrogen bonds involved in antigen-antibody complementary association requires both structural and thermodynamic information. Yokota *et al* examined the interaction between HEL and its HyHEL-10 variable domain fragment (Fv) antibody [28]. They constructed three antibody mutants and investigated the interactions between the mutant Fvs and HEL. The results from ITC indicate that the mutations significantly decreased the negative enthalpy change, despite some offset by a favorable entropy change. X-ray crystallography demonstrate that the complexes have nearly identical structures, including the positions of the interfacial water molecules. Together, the ITC and X-ray crystallographic results indicate that hydrogen bonding via interfacial water enthalpically contributes to the Fv-HEL interaction despite the partial offset because of entropy loss, suggesting that hydrogen bonding stiffens the antigen-antibody complex [28].

ITC Applications in Protein-DNA/RNA Interactions

ITC has been used to study problems related to DNA and RNA biochemistry. There have been several works in the area of protein-DNA/RNA interactions [29–34]. Gel shift assays and size exclusion column studies are probably the most common methods used to analyze DNA/RNA-protein interactions because of their relative simplicity and their small sample preparations. However, ITC provides some other advantages. The fast and automated machine can provide direct thermodynamic information of enthalpy change, entropy change, stoichiometry and binding constant.

Minetti *et al* employed ITC to investigate the binding of a bifunctional repair enzyme, *Escherichia coli* formamidopyrimidine-glycosylase (Fpg) to a series of 13-mer DNA duplexes as an initial step in defining the thermodynamic profile of glycosylase-mediated DNA repair [29]. The ITC-binding studies were carried out between 5 ºC and 15 ºC, and indicate that binding free energies are relatively independent of temperature while the reaction enthalpy and entropy are strongly temperature-dependent. The interaction is exclusively an entropy-driven process that is characterized by a strongly unfavorable binding enthalpy. The large negative heat capacity of the binding interaction is consistent with Fpg complexation to the THF-containing duplexes involving significant burial of non-polar surface areas. The structural and energetic information from the thermodynamic investigations between Fpg and DNA duplexes have led to a better understanding of the molecular forces that modulate lesion recognition and repair [29].

Buczek *et al* measured the stoichiometry, enthalpy change, entropy change and dissociation constant for binding telomere DNA fragments with the α protein N-terminal domain at different temperatures and salt concentrations using ITC [30]. Several telomere DNA fragments were synthesized, and thermodynamic parameters of the binding to them of α subunit of the telomere end-binding protein were reported. Their results show that each fragment forms a monovalent protein complex with the protein except for the fragment d(T4G4T4G4), which has two tandemly repeated d(TTTTTGGGG) telomere motifs with a high-affinity binding site and a low-affinity binding site. The relative contributions of entropy change and enthalpy change for binding reactions are DNA length-dependent, as is negative heat capacity change. These results are important for understanding early intermediate and subsequent stages in the assembly of the full telomere nucleoprotein complex and how binding events can prepare the telomere DNA for extension by telomerase, a critical event in telomere biology [30].

Using ITC, Ziegler *et al* observed that HIV-1 Tat (47–57) [31], a cell-penetrating peptide (CPP), has a high affinity for double-stranded salmon sperm DNA, as characterized by a dissociation constant of 126 nM. The observed dissociation constant for binding of HIV-1 Tat-PTD to DNA was only slightly higher than that for the specific interaction

of the full-length HIV-1 Tat to TAR, which confers stability to the uptake complexes of extracellular DNA and CPPs, and also points to the potential interference of the CPP with intracellular DNA as well as the competitive release of the cargo after cellular uptake. The binding is exothermic, and the dissociation constant and reaction enthalpy decrease further at higher temperatures. The high value of entropy likely reflects the release of hydration water and counter-ions during polyelectrolyte binding and condensation, which light-scattering data also support. Both favorable negative enthalpy and favorable positive entropy drive the binding reaction, and they are even more favorable at higher temperatures [31].

ITC analyses of the binding of human cytomegalovirus DNA polymerase UL44 to several different double-stranded DNA have been characterized by Loregian *et al* [32]. UL44 binds to DNA as a dimer, and that binding is entropically driven, while the dependence of binding on DNA length exists, which are consistent with the results of electrophoretic mobility shift assays. They have also suggested a minimum DNA length for UL44 interactions. The thermodynamic investigation has furthered understanding of how the human cytomegalovirus DNA polymerase accessory protein interacts with DNA and has also provided some insight into its mechanism of processivity [32].

Recht *et al* determined thermodynamics of the cooperativity in the assembly of the central domain from the 30S rRNA subunit of *A. aeolicus* by ITC [33]. They observed that there is cooperativity in the binding of S15, S6 and S18, but binding of S8 and S11 is independent of all other proteins from the enthalpy of each binding event. These results suggest that interdependencies of protein binding in the assembly of the *A. aeolicus* central domain are similar, but not identical, to those observed in the *E. coli* assembly map [33].

Volpon *et al* carried out ITC experiments to detect a short single-stranded RNA binding with TcUBP1 [34], a trypanosome cytoplasmic RNA-binding protein containing a single and conserved RNA-recognition motif domain involved in selective destabilization of U-rich mRNAs. The RNA binding reaction was driven by a large negative enthalpy change, suggesting the formation of hydrogen bonds, van der Waals contacts, and/or electrostatic interactions. Given the polar and charged nature of RNA, it is likely that hydrogen-bond/electrostatic interactions contribute significantly to the binding reaction. A large negative entropy change accompanied the binding events, indicating an increase in order during the RNA binding due to the reduction in the translational and rotational degrees of freedom of the RNA and the protein side chains engaged in complex formation [34].

ITC Applications in Protein-small Molecule Interactions

An understanding of the molecular basis of protein-small molecule interactions is crucial to attempts to design novel drug technologies. The thermodynamic information of the interactions of protein-small molecule obtained from ITC facilitates the understanding of the binding modes and is helpful to the development of novel drugs for some serious diseases [35–41].

Ferulic acid (FA) is one of the most effective components of the traditional Chinese medicine *Angelica*, and cytochrome *c* plays a vital role in apoptosis. We reported the application of ITC and several biophysical methods to investigate the mechanism for the interaction between bovine heart cytochrome *c* and FA as well as the effect of the binding on native state stability of the protein at physiological pH [35]. ITC studies together with fluorescence spectroscopic measurements indicate that FA binds to cytochrome *c* with moderate affinity and quenches the intrinsic fluorescence of the protein in a static way. The interaction of cytochrome *c* with FA is driven by a moderately favorable entropy increase in combination with a less favorable enthalpy decrease for the first binding site of the protein. The melting temperature of cytochrome *c* in the presence of FA measured by differential scanning calorimetry and circular dichroism increases 4 ºC and 5 ºC respectively, compared with that in the absence of FA. Taken together, these results indicate that FA binds to and stabilizes cytochrome *c* at physiological pH. Furthermore, binding of FA to cytochrome *c* inhibits cytochrome *c*-induced apoptosis of human hepatoma cell line SMMC-7721. Our data provide insight into the mechanism of drug-protein interactions and will be helpful in understanding the mechanism for FA-inhibited and cytochrome *c*-induced apoptosis [35].

Bicyclomycin is the only natural product inhibitor with weak binding affinity of the transcription termination factor rho, which is a hexameric helicase that terminates nascent RNA transcripts utilizing ATP hydrolysis and is an essential protein for many bacteria. Brogan *et al* determined the information concerning a bicyclomycin analogue-rho interaction using ITC [36]. Their study found that a designed bicyclomycin ligand, 5a-(3-formyl-phenylsulfanyl)-dihydrobicyclomycin, inhibits rho an order of magnitude more efficiently than bicyclomycin [36].

Organisms rely heavily on protein phosphorylation to transduce intracellular signals. The phosphorylation of a

protein often induces conformational changes, which are responsible for triggering downstream cellular events. Engel *et al* developed some specific, low molecular weight compounds that target the hydrophobic motif/PIF-pocket and have the ability to allosterically activate phosphoinositide-dependent protein kinase 1 (PDK1) by modulating the phosphorylation-dependent conformational transition [37]. The interaction of compound 1 with PDK1 was studied using ITC, and the experiments indicate that compound 1 binds to PDK1 CD with a 1:1 stoichiometry and a binding affinity in the micromolar range. These results raise the possibility of developing drugs that target the AGC kinases via a novel mode of action and may inspire future rational development of compounds with the ability to modulate phosphorylation-dependent conformational transitions in other proteins [37].

An efficient research strategy integrating empirically guided, structure-based modeling and chemoinformatics was used to discover potent small molecule inhibitors of the botulinum neurotoxin serotype A (botulinum A) light chain. Using ITC, Burnett *et al* studied the interaction between a small molecule NSC 240898 and the botulinum A light chain [38]. The inhibitor interaction with the botulinum A light chain is a low affinity binding event with a 1:1 stoichiometry. Furthermore, the interaction is largely entropy-driven, and the enthalpic component is relatively low. The substantial entropic contribution to the binding event suggests a burial of hydrophobic surfaces and the release of solvent [38].

The *E. coli* isocitrate lyase regulator (IclR) regulates the expression of the glyoxylate bypass operon. IclR comprises a DNA binding domain that interacts with the operator sequence and a C-terminal domain that binds a hitherto unknown small molecule. Glyoxylate and pyruvate, identified by Lorca *et al*, bind to the C-IclR domain, as defined by ITC [39]. The titration of C-IclR with each compound followed an exothermal heat change profile, giving rise to a sigmoidal binding curve with glyoxylate or hyperbolic with pyruvate. The stoichiometry of the reaction, 0.5, was consistent with the binding of one ligand molecule per IclR dimer. In accordance with other results, the C-IclR dissociation constant for glyoxylate was significantly lower than that for pyruvate. In general, their strategy of combining chemical screens with functional assays and structural studies has uncovered two small molecules with antagonistic effects that regulate the IclR-dependent transcription of the *aceBAK* operon [39].

Organisms commit a considerable amount of genetic and metabolic resources to managing metal ions. This involves proteins dedicated to the uptake, transport, storage and export of essential metal as well as their delivery to proteins and enzymes requiring one or more metals for their stability and/or catalytic activity [40]. A review by Wilcox highlighted many of the recent studies of metal ions binding to proteins that have used ITC to quantify the thermodynamics of metal-protein interactions [40].

The cellular prion protein is known to be a copper-binding protein. Thompsett *et al* used two techniques, ITC and competitive metal capture analysis, to determine the affinity of copper for wild-type mouse PrP and a series of mutants [41]. High affinity copper binding by wild-type PrP was confirmed by independent techniques, which indicated the presence of specific tight copper binding sites up to femtomolar affinity. Altogether, four high affinity binding sites of between femto- and nanomolar affinities were located within the octameric repeat region of the protein at physiological pH. A fifth copper binding site of lower affinity than those of the octameric repeat region was detected in full-length protein. Binding to this site is modulated by the histidine at residue 111. Removal of the octameric repeats led to the enhancement of affinity of this fifth site and a second binding site outside of the repeat region undetected in the wild-type protein. High affinity copper binding allows PrP to compete effectively for copper in the extracellular milieu. The copper binding affinities of PrP were compared with those of proteins of known function, and they are of magnitudes compatible with an extracellular copper buffer or an enzymatic function, such as superoxide dismutase-like activity [41].

Reverse Titration of ITC

The injected reactant located in the syringe is referred to as "ligand". Usually small molecules should be placed in the syringe, and the targeted protein should be placed in the cell. Sometimes reverse titrations (i.e., reversing the role of macromolecule and ligand) are conducted to check the stoichiometry or the suitability of the binding model [42].

In the present study, I have used reverse titration of ITC to measure the binding affinity of oleic acid to Ca^{2+}-depleted bovine α-lactalbumin (apo-BLA). A reverse titration of 287 μM apo-BLA into 36 μM oleic acid using 28×10-μl injections was performed because of the insolubility of oleic acid, and the ITC results are shown in **Fig. 2(A,B)**. The best fit for the integrated heat data was obtained using a three sequential-binding sites model, yielding the thermodynamic parameters for the interaction between apo-BLA and oleic acid: $K_{b,1}=(1.02\pm0.25)\times10^5\ M^{-1}$, $\Delta_b H^0_{m,1}=32.1\pm3.1$ kcal·mol^{-1}, $\Delta_b G^0_{m,1}=-7.10\pm0.15$

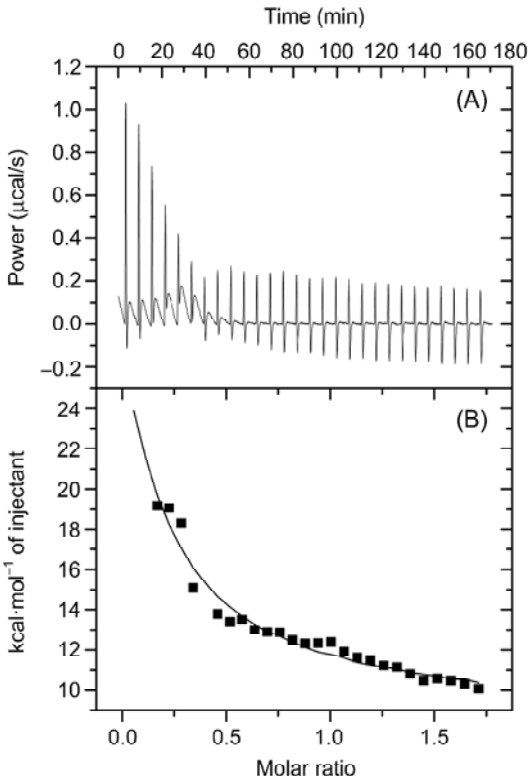

Fig. 2 Reverse isothermal titration calorimetry profile of Ca^{2+}-depleted bovine α-lactalbumin (apo-BLA) titrated into a solution of oleic acid (A) The raw data for sequential 10-μl injections of 287 M apo-BLA into 36 μM oleic acid in 10 mM ammonium acetate buffer (pH 4.3) at 37 ºC. (B) The plot of the heat evolved (kcal) per mole of apo-BLA added, corrected for the heat of apo-BLA dilution, against the molar ratio of apo-BLA to oleic acid. The data (solid squares) were fitted to a three sequential-binding sites model, and the solid lines represent the best fit.

kcal·mol^{-1}, $\Delta_b S^0_{m,1}$ =126±11 cal·mol^{-1}·K^{-1}, $K_{b,2}$=(0.98±0.19)×10^5 M^{-1}, $\Delta_b H^0_{m,2}$ =–18.2±5.6 kcal·mol^{-1}, $\Delta_b G^0_{m,2}$ = –7.08±0.12 kcal·mol^{-1}, $\Delta_b S^0_{m,2}$ =–35.9±18.5 cal·mol^{-1}·K^{-1}, $K_{b,3}$=(0.98±0.29)×10^5 M^{-1}, $\Delta_b H^0_{m,3}$ =38.2±6.5 kcal·mol^{-1}, $\Delta_b G^0_{m,3}$ =–7.08±0.18 kcal·mol^{-1}, and $\Delta_b S^0_{m,3}$ =146±21 cal·mol^{-1}·K^{-1}. Our results show that the binding of oleic acid to apo-BLA is driven entirely by large favorable entropy increases but with unfavorable enthalpy increases for the first and the third sequential-binding sites of nonnative lysozyme. The oscillating calorimetric signal indicates the formation of the aggregates of apo-BLA induced by oleic acid.

To characterize driving forces and driven processes in the formation of a large interface, wrapped protein-DNA complex analogous to the nucleosome, Vander Meulen *et al* investigated the thermodynamics of binding the 34 bp H' DNA sequence to the *E. coli* DNA-remodeling protein integration host factor (IHF) [43]. Thermodynamic parameters for integration host factor-H' DNA interactions were determined by ITC from forward and reverse titrations. Both the binding constant and the binding enthalpy depend strongly on salt concentration and anion identity. Formation of the wrapped complex is enthalpy driven, especially at a low concentration of salt [43].

The HIV-1 nucleocapsid (NC) protein is a small, basic protein containing two retroviral zinc fingers. NC binds with high-affinity to the repeating sequence d(TG)n. The interactions between NC and $(TG)_4$ have been characterized by ITC [44]. The forward titration curve reaches saturation at a molar ratio of approximately 1.0. A reverse titration in which NC was titrated into a solution of 10 mM $(TG)_4$ was also performed, but no clear saturation was observed. The dependence of the total heat released upon the direction of the titration also underscores the complexity of the interactions between NC and $(TG)_4$. The role of electrostatic interactions in the binding was probed, both by repeating the titration of NC into $(TG)_4$ in varying concentrations of NaCl and by using the "N-term" mutant protein. The amount of heat released was drastically reduced in both of these experiments, suggesting that that Coulombic attractions play a major role in the interactions between NC and $(TG)_4$ [44].

Displacement Method of ITC

An important goal in drug development is to engineer inhibitors and ligands that have high binding affinities for their target molecules. In optimizing these interactions, the precise determination of the binding affinity becomes progressively difficult once it approaches and surpasses the nanomolar level. ITC can be used to determine the complete binding thermodynamics of a ligand down to the picomolar range by using an experimental mode called displacement titration, a new and important progress in ITC [42]. In the recent years, this displacement method has been applied successfully in calorimetry when dealing with very high or very low affinity systems [42,45]. This method is based on the fact that the binding properties of a ligand are altered when another competing ligand is present.

In a displacement titration, the association constant of a high-affinity ligand that cannot be measured directly is artificially lowered to a measurable level by premixing the protein with a weaker competitive ligand. To perform this protocol, three titrations must be carried out: a direct titration of the high-affinity ligand to the target protein, a

direct titration of the weak ligand to the target protein and a displacement titration of the high-affinity ligand to the weak ligand-target protein complex [42]. In a displacement titration, the weak competitive ligand must be present in the calorimetric cell at a concentration sufficient to reduce the affinity of the high-affinity ligand to measurable levels ($K_a \leq 10^9$ M^{-1}). The apparent binding affinity of the high-affinity ligand, K_L^{app}, is reduced by a factor, RF, dependent on the binding affinity, K_{aX}, and the concentration of the weak ligand [42]:

$$K_L^{app} = \frac{K_{a,L}}{RF} = \frac{K_{a,L}}{1+K_{a,X}[X]}$$

where [X] is the concentration of the free weak ligand X, which is unknown. For practical purposes, the total concentration of a weak ligand required to achieve a predetermined reduction factor is approximately [42]:

$$[X]_T = \frac{RF\text{-}1}{K_{a,X}} + [M]_T$$

where $[X]_T$ and $[M]_T$ are the total weak ligand and total macromolecule concentration in the calorimetric cell. The displacement method of ITC has been used successfully to determine the binding constant of a high-affinity HIV-1 protease inhibitor using acetyl-pepstatin as the weak inhibitor [42].

If we are interested in characterizing a very low affinity ligand, then a moderate affinity ligand is used as competing ligand and a thermodynamic principle similar to the above is used [45]. Three titrations are performed: a direct titration of moderate affinity ligand into the protein solution, from which the both the binding affinity and the binding enthalpy can be obtained; a direct titration of low affinity ligand into the protein solution, from which neither the binding affinity nor the binding enthalpy can be reliably obtained; and displacement titration of moderate affinity ligand A into a solution of macromolecule and ligand B [45].

In the work of Andújar-Sánchez *et al* [46], the binding constants of angiotensin-converting enzyme inhibitors were determined by a displacement method of ITC. Somatic angiotensin I-converting enzyme (s-ACE) plays a central role in blood pressure regulation and has been the target of most antihypertensive drugs. Direct ITC titrations were made to determine binding enthalpy and binding constants for L-Asp-L-Phe. Binding constants for the strong inhibitors, captopril, lisinopril and enalaprilat, were measured by the displacement method. For each displacement experiment, a solution of s-ACE was first titrated until saturation with the weak inhibitor L-Asp-L-Phe. Then, the injection syringe was cleaned and refilled with a solution of the strong inhibitor to perform a second titration. The relative potency of the inhibitors was determined to be enalaprilat>lisinopril>captopril. Andújar-Sánchez *et al* analyzed the thermodynamic behavior of the binding process using the new structural information provided by the ACE structures, as well as the conformational changes that occurred upon binding [46].

Conclusions

The ITC method is gaining wider usage with respect to investigating protein interactions in signal transduction and deeper usage with respect to investigating protein folding and misfolding. The proliferation of this method in academic and industrial laboratories has produced a lot of new reports of interesting applications, new systems studied and advances in data analyses. Here, the new application of ITC in protein folding and misfolding, as well as its traditional application in protein interactions is reviewed. From analyzing the experimental data, scientists have gained a better understanding of the relationships between the ITC data and structural details. Methods for analyzing ITC still need to be further developed to ensure the effectiveness of ITC results. Combining X-ray crystallography and nuclear magnetic resonance spectroscopy with ITC may be one method that will help provide greater understanding of the complexities of protein folding and protein interactions.

References

1 Cliff MJ, Gutierrez A, Ladbury JE. A survey of the year 2003 literature on applications of isothermal titration calorimetry. J Mol Recognit 2004, 17: 513–523
2 Ababou A, Ladbury JE. Survey of the year 2004: literature on applications of isothermal titration calorimetry. J Mol Recognit 2006, 19: 79–89
3 Ababou A, Ladbury JE. A survey of the year 2005 literature on applications of isothermal titration calorimetry. J Mol Recognit 2007, 20: 4–14
4 Okhrimenkoa O, Jelesarov I. A survey of the year 2006 literature on applications of isothermal titration calorimetry. J Mol Recognit 2008, 21: 1–19
5 Baker BM, Murphy KP. Evaluation of linked protonation effects in protein binding reactions using isothermal titration calorimetry. Biophys J 1996, 71: 2049–2055
6 Connelly PR, Varadarajan R, Sturtevant JM, Richards FM. Thermodynamics of protein-peptide interactions in the ribonuclease S system studied by titration calorimetry. Biochemistry 1990, 29: 6108–6114
7 Spolar RS, Record MT Jr. Coupling of local folding to site-specific binding of proteins to DNA. Science 1994, 263: 777–784
8 Anfinsen CB. Principles that govern the folding of protein chains.

Science 1973, 181: 223–230
9 Liang Y, Du F, Sanglier S, Zhou BR, Xia Y, Van Dorsselaer A, Maechling C *et al*. Unfolding of rabbit muscle creatine kinase induced by acid. A study using electrospray ionization mass spectrometry, isothermal titration calorimetry, and fluorescence spectroscopy. J Biol Chem 2003, 278: 30098–30105
10 Fan YX, Zhou JM, Kihara H, Tsou CL. Unfolding and refolding of dimeric creatine kinase equilibrium and kinetic studies. Protein Sci 1998, 7: 2631–2641
11 Nakamura S, Kidokoro S. Direct observation of the enthalpy change accompanying the native to molten-globule transition of cytochrome c by using isothermal acid-titration calorimetry. Biophys Chem 2005, 113: 161–168
12 Luke K, Wittung-Stafshede P. Folding and assembly pathways of co-chaperonin proteins 10: Origin of bacterial thermostability. Arch Biochem Biophys 2006, 456: 8–18
13 Yang F Jr, Zhang M, Zhou BR, Chen J, Liang Y. Oleic acid inhibits amyloid formation of the intermediate of α-lactalbumin at moderately acidic pH. J Mol Biol 2006, 362: 821–834
14 Kardos J, Yamamoto K, Hasegawa K, Naiki H, Goto Y. Direct measurement of the thermodynamic parameters of amyloid formation by isothermal titration calorimetry. J Biol Chem 2004, 279: 55308–55314
15 Zhou BR, Liang Y, Du F, Zhou Z, Chen J. Mixed macromolecular crowding accelerates the oxidative refolding of reduced, denatured lysozyme: implications for protein folding in intracellular environments. J Biol Chem 2004, 279: 55109–55116
16 Du F, Zhou Z, Mo ZY, Shi JZ, Chen J, Liang Y. Mixed macromolecular crowding accelerates the refolding of rabbit muscle creatine kinase: implications for protein folding in physiological environments. J Mol Biol 2006, 364: 469–482
17 Zhou BR, Zhou Z, Hu QL, Chen J, Liang Y. Mixed macromolecular crowding inhibits amyloid formation of hen egg white lysozyme. Biochim Biophys Acta 2008, 1784: 472–480
18 Ahmad MF, Ramakrishna T, Raman B, Rao ChM. Fibrillogenic and non-fibrillogenic ensembles of SDS-bound human α-synuclein. J Mol Biol 2006, 364: 1061–1072
19 Groenning M, Norrman M, Flink JM, van de Weert M, Bukrinsky JT, Schluckebier G, Frokjaer S. Binding mode of thioflavin T in insulin amyloid fibrils. J Struct Biol 2007, 159: 483–497
20 Zhou YL, Liao JM, Chen J, Liang Y. Macromolecular crowding enhances the binding of superoxide dismutase to xanthine oxidase: implications for protein-protein interactions in intracellular environments. Int J Biochem Cell Biol 2006, 38: 1986–1994
21 Zhou YL, Liao JM, Chen J, Liang Y. Thermodynamics of the interaction of xanthine oxidase with superoxide dismutase by isothermal titration calorimetry and fluorescence spectroscopy. Thermochim Acta 2005, 426: 173–178
22 Jin R, Rummel A, Binz T, Brunger AT. Botulinum neurotoxin B recognizes its protein receptor with high affinity and specificity. Nature 2006, 444: 1092–1095
23 Knipscheer P, van Dijk WJ, Olsen JV, Mann M, Sixma TK. Noncovalent interaction between Ubc9 and SUMO promotes SUMO chain formation. EMBO J 2007, 26: 2797–2807
24 Chen Y, Xu Y, Bao Q, Xing Y, Li Z, Lin Z, Stock JB *et al.* Structural and biochemical insights into the regulation of protein phosphatase 2A by small t antigen of SV40. Nat Struct Mol Biol 2007, 14: 527–534
25 Rainaldi M, Yamniuk AP, Murase T, Vogel HJ. Calcium-dependent and -independent binding of soybean calmodulin isoforms to the calmodulin binding domain of tobacco MAPK phosphatase-1. J Biol Chem 2007, 282: 6031–6042
26 Kiel C, Selzer T, Shaul Y, Schreiber G, Herrmann C. Electrostatically optimized Ras-binding Ral guanine dissociation stimulator mutants increase the rate of association by stabilizing the encounter complex. Proc Natl Acad Sci U S A 2004, 101: 9223–9228
27 Siligardi G, Hu B, Panaretou B, Piper PW, Pearl LH, Prodromou C. Co-chaperone regulation of conformational switching in the Hsp90 ATPase cycle. J Biol Chem 2004, 279: 51989–51998
28 Yokota A, Tsumoto K, Shiroishi M, Kondo H, Kumagai I. The role of hydrogen bonding via interfacial water molecules in antigen-antibody complexation. The HyHEL-10-HEL interaction. J Biol Chem 2003, 278: 5410–5418
29 Minetti CA, Remeta DP, Zharkov DO, Plum GE, Johnson F, Grollman AP, Breslauer KJ. Characterization of formamidopyrimidine-glycosylase(Fpg) interactions with damaged DNA duplexes. J Mol Biol 2003, 328: 1047–1060
30 Buczek P, Horvath MP. Thermodynamic characterization of binding *Oxytricha nova* single strand telomere DNA with the alpha protein N-terminal domain. J Mol Biol 2006, 359: 1217–1234
31 Ziegler A, Seelig J. High affinity of the cell-penetrating peptide HIV-1 Tat-PTD for DNA. Biochemistry 2007, 46: 8138–8145
32 Loregian A, Sinigalia E, Mercorelli B, Palù G, Coen DM. Binding parameters and thermodynamics of the interaction of the human cytomegalovirus DNA polymerase accessory protein, UL44, with DNA: implications for the processivity mechanism. Nucleic Acids Res 2007, 35: 4779–4791
33 Recht MI, Williamson JR. RNA tertiary structure and cooperative assembly of a large ribonucleoprotein complex. J Mol Biol 2004, 344: 395–407
34 Volpon L, D'Orso I, Young CR, Frasch AC, Gehring K. NMR structural study of TcUBP1, a single RRM domain protein from *Trypanosoma cruzi*: contribution of a β hairpin to RNA binding. Biochemistry 2005, 44: 3708–3717
35 Yang F, Zhou BR, Zhang P, Zhao YF, Chen J, Liang Y. Binding of ferulic acid to cytochrome c enhances stability of the protein at physiological pH and inhibits cytochrome c-induced apoptosis. Chem Biol Interact, 2007, 170: 231–243
36 Brogan AP, Widger WR, Bensadek D, Riba-Garcia I, Gaskell SJ, Kohn H. Development of a technique to determine bicyclomycin-rho binding and stoichiometry by isothermal titration calorimetry and mass spectrometry. J Am Chem Soc 2005, 127: 2741–2751
37 Engel M, Hindie V, Lopez-Garcia LA, Stroba A, Schaeffer F, Adrian I, Imig J *et al*. Allosteric activation of the protein kinase PDK1 with low molecular weight compounds. EMBO J 2006, 25: 5469–5480
38 Burnett JC, Ruthel G, Stegmann CM, Panchal RG., Nguyen TL, Hermone AR, Stafford RG *et al*. Inhibition of metalloprotease botulinum serotype A from a pseudo-peptide binding mode to a small molecule that is active in primary neurons. J Biol Chem 2007, 282: 5004–5014
39 Lorca GL, Ezersky A, Lunin VV, Walker JR, Altamentova S, Evdokimova E, Vedadi M *et al*. Glyoxylate and pyruvate are antagonistic effectors of the *Escherichia coli* IclR transcriptional regulator. J Biol Chem 2007, 282: 16476–16491
40 Wilcox DE. Isothermal titration calorimetry of metal ions binding to proteins: an overview of recent studies. Inorganica Chim Acta 2008, 361: 857–867
41 Thompsett AR, Abdelraheim SR, Daniels M, Brown DR. High affinity binding between copper and full-length prion protein iden-

tified by two different techniques. J Biol Chem 2005, 280: 42750–42758

42 Velazquez-Campoy A, Freire E. Isothermal titration calorimetry to determine association constants for high-affinity ligands. Nat Protoc 2006, 1:186–191

43 Vander Meulen KA, Saecker RM, Record MT Jr. Formation of a wrapped DNA-protein interface: experimental characterization and analysis of the large contributions of ions and water to the thermodynamics of binding IHF to H' DNA. J Mol Biol 2008, 377: 9–27

44 Fisher RJ, Fivash MJ, Stephen AG, Hagan NA, Shenoy SR, Medaglia MV, Smith LR *et al*. Complex interactions of HIV-1 nucleocapsid protein with oligonucleotides. Nucleic Acids Res 2006, 34: 472–484

45 Velázquez Campoy A, Freire E. ITC in the post-genomic era…? Priceless. Biophys Chem 2005, 115: 115–124

46 Andújar-Sánchez M, Jara-Pérez V, Cámara-Artigas A. Thermodynamic determination of the binding constants of angiotensin-converting enzyme inhibitors by a displacement method. FEBS Lett 2007, 581: 3449–3454